Mechanical Properties of Different Anatomical Sites of the Bone-Tendon Origin of Lateral Epicondyle

Jung Soo Han*
Department of Mechanical and Systems Engineering, CSST, Hansung University, Seoul 136-792, Korea

A series of rabbit common extensor tendon specimens of the humeral epicondyle were subjected to tensile tests under two displacement rates (100 mm/min and 10 mm/min) and different elbow flexion positions 45°, 90° and 135°. Biomechanical properties of ultimate tensile strength, failure strain, energy absorption and stiffness of the bone-tendon specimen were determined. Statistically significant differences were found in ultimate tensile strength, failure strain, energy absorption and stiffness of bone-tendon specimens as a consequence of different elbow flexion angles and displacement rates. The results indicated that the bone-tendon specimens at the 45° elbow flexion had the lowest ultimate tensile strength; this flexion angle also had the highest failure strain and the lowest stiffness compared to other elbow flexion positions. In comparing the data from two displacement rates, bone-tendon specimens had lower ultimate tensile strength at all flexion angles when tested at the 10 mm/min displacement rate. These results indicate that creep damage occurred during the slow displacement rate. The major failure mode of bone-tendon specimens during tensile testing changed from 100% of midsubstance failure at the 90° and 135° elbow flexion to 40% of bone-tendon origin failure at 45°. We conclude that failure mechanics of the bone-tendon unit of the lateral epicondyle are substantially affected by loading direction and displacement rate.

Key Words : Mechanical Properties, Bone-Tendon Origin, Epicondyle Common Extensor, Failure Mechanics

1. Introduction

Based on clinical and surgical evidence, microtear, microfailure or partial failure at the bone-tendon junction or musculo-tendinous junction, most often occurring within the origin of the extensor carpi radialis brevis, acts as the initiator of epicondylitis (Nirshcl, 1973; Jobe, *et al.*, 1994). Biomechanical studies have demonstrated that forceful exertions can produce stress concentrations on tendons and adjacent tissues that correspond with the sites of injury (Armstrong *et al.*, 1979a; Castelli *et al.*, 1980).

The common extensor tendon of the humeral epicondyle is a crucial structure in the elbow and has not been subjected to intense biomechanical studies, partly due to its complicated structure and the testing difficulties with the limited length of bone-tendon specimen. Our laboratory has recently developed an experimental device whereby the bone-tendon specimen can be oriented and tested at any desired loading direction. Previous work in our lab characterized failure strength of human common extensor and flexor tendons of the humeral epicondyle (Han *et al.*, 1994). Results from this work convinced us that failure occurred at the bone-tendon junction of the epicondyle under either loading condition (slow or fast displacement rates). Wang *et al.* (1995)

* Corresponding Author,
E-**mail** : jshan@hansung.ac.kr
TEL : +82-2-760-4323 ; **FAX** : +82-2-760-4329
Department of Mechanical and Systems Engineering, CSST,Hansung University, 389 Samsun-dong, Sungbuk-gu, Seoul 136-792, Korea.

has recently conducted a study to determine biomechanical properties, such as ultimate tensile strength, failure strain and elastic modulus, of bone-tendon specimens of human common extensor tendons under different loading directions. Results from this study indicated that different directions of load application resulted in different mechanical responses in the bone-tendon specimen of the humeral epicondyle. However, due to the limited number of human specimens and other variables, such as age and personal history, the results could not demonstrate the mechanical properties of the bone-tendon unit of humeral epicondyhle completely.

The present study was undertaken to evaluate the effect of the direction of applied load and displacement rate on the mechanical properties (ultimate tensile strength, failure strain, energy absorption and linear stiffness) of bone-tendon specimens of the rabbit humeral epicondyle. Because the common extensor tendon and its insertion site are viscoelastic and are not homogeneous, but rather a composite material (Wainwright, 1976; Currey, 1984), it was hypothesized that different directions of load application and different displacement rate would result in different mechanical responses and failure patterns in tendons and at the bone-tendon junction. To examine this hypothesis, experimental force-displacement data were obtained for the rabbit common extensor tendon of the humeral epicondyle when loaded to failure in various directions at two different displacement rates. From these data, values were determined for ultimate tensile strength and failure mode of the bone-tendon specimen. Failure strain, energy absorption and stiffness for tendon and the bone-tendon junction were also determined.

2. Materials and Methods

Thirty-six New Zealand white rabbits (seventy-two common extensor tendon specimens) of similar ages and both sexes, weighing 3.5 to 4.5 kilograms, were used. Each animal was sacrificed using and intracardiac injection of sodium pentobarbital and both forelimbs were disarticulated. The limbs were wrapped in plastic bags and stored at $-15℃$. Before testing, specimens were removed from the freezer and thawed at room temperature. Anterior-posterior and lateral roentgenograms excluded specimens with bony abnormality. All muscles, except the common extensor tendon and the origin of the epicondyle, were removed. Approximately 40 mm of the common extensor tendon, distally from its origin, remained after dissection. A custom-designed grip device held the tendon 15 mm distal to its origin at the humeral epicondyle. The grip device was placed into the test fixture and attached to a servo hydraulic materials testing system (MTS) with the distal part of the tendon at the selected angle of flexion. The loading fixture was oriented such that the direction of loading was along the anatomical position of elbow flexion. Specimens were kept moist with physiological saline throughout preparation and testing. Mechanical testing was performed at room temperature.

2.1 Experimental apparatus

Mechanical tests were performed on the MTS machine. Prepared specimens were mounted with bone cement in an electrical conduit 10 mm in diameter. Custom-designed devices attached to the MTS machine made it possible to change the elbow flexion angle (45°, 90° and 135°). For tensile tests, load and displacement were monitored with a load cell and a linear variable displacement transducer (LVDT), respectively. Data for ultimate tensile strength from the bone-tendon specimens was collected by a personal computer using Labtech Notebook software (Labtech, wilmington, MA).

Strain measurements in tendon and bone were recorded using two differential variable reluctance transducers (DVRT) which were fixed to the tendon and bone in a straight line representing the loading direction. Two ultra fine wires were separately welded to the top surface of the DVRT in the tendon and the bottom surface of the DVRT in the bone to establish the gauge length for the bone-tendon complex. The strain for the bone-tendon complex was obtained using a video motion analysis system, consisting of

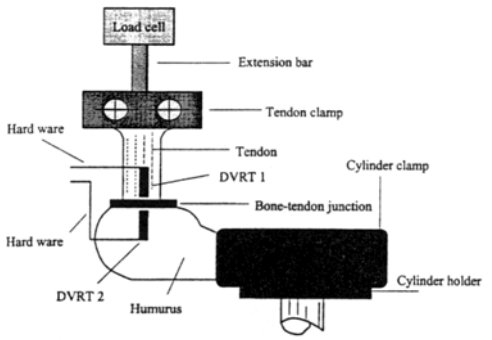

Fig. 1 Schematic diagram of the Rabbit bone-tendon specimen during a tensile test

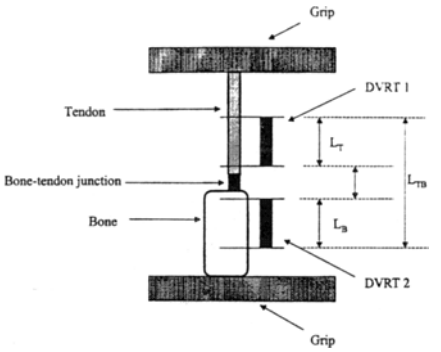

Fig. 2 Schematic diagram of strains measuring system

COHU solid state camera, AL16, fitted with a Monocular/45 Field microscope, JVC video tape recorder, HR-6700U and Sony monitor, to record changes of the gauge length between the two wires (Fig. 1). The video recording can be played back at slow speed into an optimas imaging system (Edmonds, WA), which includes an Olympus BH-2 with bright and dark field illumination and a Dell 90 MHX pentium computer with a Matrox MVPAT image capture board. It automatically identifies points, lines and distances between the ultra fine wires. The data was recorded and transferred to Excel.

Data were analyzed using a two-way analysis of variance (ANOVA) to determine any statistically significant difference ($p<0.05$) in ultimate tensile strength, failure strain and linear stiffness due to varied loading directions, displacement rates and anatomic sites (tendon versus the bone-tendon junction).

2.2 Experimental procedure

Thirty-six rabbits were divided into two groups. Specimens in one group were loaded to failure at a displacement rate of 10 mm/min and the second group was tested at 100 mm/min. Each group was divided into three subgroups which were loaded in different elbow flexion positions of 45°, 90° and 135°. Twelve paired specimens in each group were loaded at 45° on one side and at 135° on other side. The rest of specimens in each group were tested at 90°.

The strain in tendon can be obtained directly from the DVRT. Strain in the bone-tendon junction has to be calculated through the strains in tendon, bone and bone-tendon complex because a large error would occur if the DEVRT was used to measure such a thin junction. Figure 2 shows the strain measuring system. The two DVRTs in tendon and bone were arranged in a straight line as close as possible. The distance, δ, in the middle represents the thickness of the bone-tendon junction. L_T, L_B and L_{TB} represent the initial length of the DVRT1 in tendon and the DVRT2 in bone and bone-tendon complex. Strain in the bone-tendon complex can be expressed:

$$\varepsilon_{TB}=\frac{L'_T+L'_B+\delta-L_{TB}}{L_{TB}} \tag{1}$$

where $L_{TB}=L_T+L_B+\delta$. Strains in the tendon, ε_T, bone, ε_B, and bone-tendon junction, ε_δ, can be expressed the follows, respectively.

$$\varepsilon_T=\frac{L'_T-L_T}{L_T},\ \varepsilon_B=\frac{L'_B-L_B}{L_B}\ \ \varepsilon_\delta=\frac{\delta'-\delta}{\delta} \tag{2}$$

therefore:

$$L'_T=L_T(\varepsilon_T+1),\ L'_B=L_B(\varepsilon_B+1),\quad \delta'=\delta(\varepsilon_\delta+1) \tag{3}$$

substitute Eq. (3) into Eq. (1). We have

$$\varepsilon_{TB}=\frac{L_T(\varepsilon_T+1)+L_B(\varepsilon_B+1)+\delta(\varepsilon_\delta+1)-L_T-T_B-\delta}{L_T+L_B+\delta} \tag{4}$$

The strain at the bone-tendon junction can be expressed with function of δ, ε_{TB}, ε_T and ε_B.

$$\varepsilon_\delta=\frac{L_T(\varepsilon_{TB}-\varepsilon_T)+L_B(\varepsilon_{TB}-\varepsilon_B)+\delta\varepsilon_{TB}}{\delta} \tag{5}$$

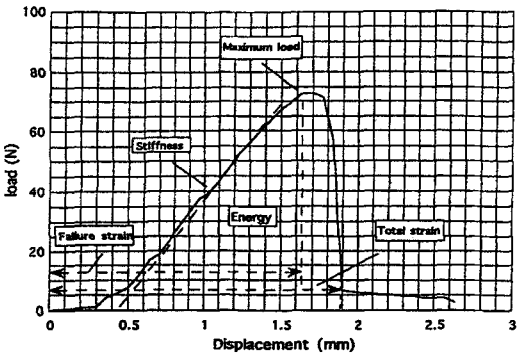

Fig. 3 An example of load versus displacement record showing behavior of the bone-tendon specimen during loading at 100 mm/min displacement rate

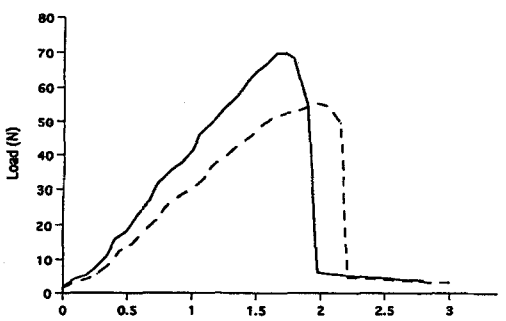

Fig. 4 Typical load-displacement curves for the bone-tendon specimens demonstating the differences in ultimate tensile strength and failure strains at displacement rates of 10 mm/min (a) and 100 mm/min (b)

2.3 Analysis of specimen behavior

Several parameters were used to characterize the behavior of each bone-tendon unit when loaded to failure: ultimate tensile strength in Newton force; strain to ultimate tensile strength and strain to complete failure; total energy to failure in millimeter-Newton force; and slope (in linear range) expressed as Newton/millimeter (Fig. 3).

3. Results

3.1 Ultimate tensile strength

The ultimate tensile strength for the specimens tested at 135° and 100 mm/min displacement rate (76.2±28.8N) was found to be 32.6% higher than that of the 90° subgroup (51.3±11.7N) and 47.1%

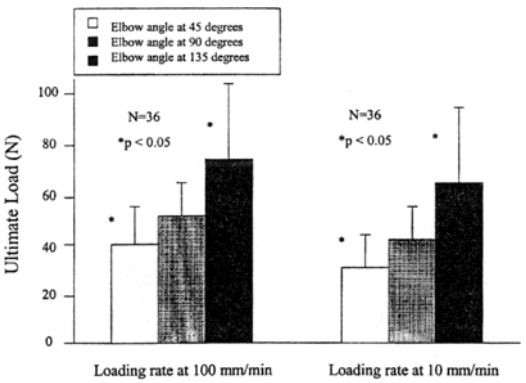

Fig. 5(a) Comparison of ultimate tensile strength at different elbow angles

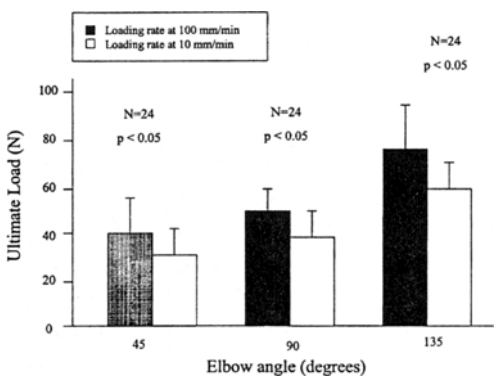

Fig. 5(b) Comparison of ultimate tensile strength at displacement rates of 10 mm/min and 100 mm/min

higher than that of the 45° subgroup (40.3±25.4N). A decrease of ultimate tensile strength related to decreasing displacement rate was seen for specimens tested at 10 mm/min. Specimen behavior at the 100 mm/min and 10 mm/min displacement rates are shown in a typical load-displacement diagram in Fig. 4. In comparing matched elbow angles at two displacement rates, the value of ultimate tensile strength at 100 mm/min rate was 30.2% higher than that for the elbow angle of 45° at 10 mm/min loading rate (28.13±15.3N), 20.5% higher than that of 90° (40.75±13.8N) and 16.8% higher than that of 135° (63.43±28.9N). Statistically, both loading direction and displacement rate had a significant effect on the ultimate tensile strength ($p<0.05$, respectively; Fig. 5(a) and Fig. 5(b)).

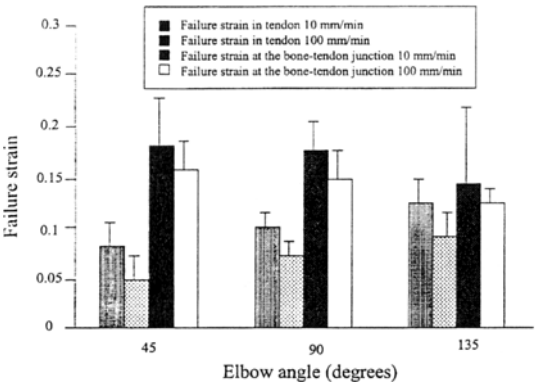

Fig. 6 Failure strains in tendon and at the bone-tendon junction at different loading directions and displacement rates

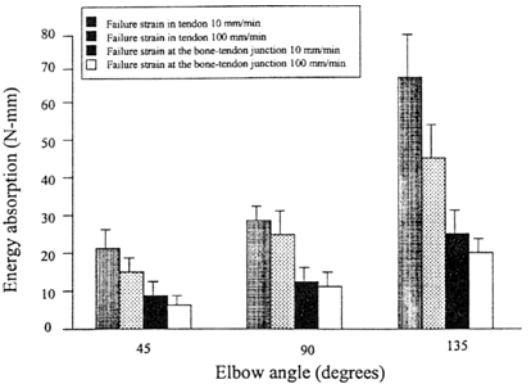

Fig. 7 Energy absorbed in tendon and at the bone-tendon junction at different loading directions and displacement rates

3.2 Failure strain

Strain values at the failure point for tendon and bone-tendon junction at both displacement rates were obtained (Fig. 6). The failure strains in tendon at oth displacement rates were affected by loading directions. Significantly higher strain values were found at 135° than at 90° and 45° ($p<0.05$). In addiction, failure strain in tendon decreased with increasing displacement rate. At 100 mm/min displacement rate, failure strains were 35.4% (45°), 28.9% (90°) and 25.8% (135°) lower than at the 10 mm/min displacement rate.

Statistically, failure strain in the bone-tendon junction did not exhibit loading direction dependency at either displacement rate ($p>0.05$). There was a significantly higher strain value at the 10 mm/min displacement rate than at 100 mm/min ($p<0.05$), indicating that the failure strain was dependent on displacement rate. In comparing failure strains in the tendon and at the bone-tendon junction, results showed that the failure strain in the bone-tendon junction was 53.9% (45°), 36.3% (90°) and 28.5% (135°) higher than in the tendon at the 10 mm/min displacement rate. At the 100 mm/min displacement rate, the failure strains in the bone-tendon junction were 220%, 200% and 150% higher than the failure strains in the tendon at 45°, 90° and 135°.

3.3 Energy absorption

The energy absorption values in the tendon followed the same trend as the failure strain in loading directions. The tendon absorbed more energy at 135° than at 90° and 45° for both displacement rates. Statistical analysis revealed that energy absorbed in the tendon was significantly affected by loading direction ($p<0.05$) and, although energy absorbed was similarly affected by displacement rates, statistical significance was not shown ($p=0.062$)

A similar trend of energy absorption was found in the bone-tendon junction as in tendon. It was approximately 38.3% higher at 135° than at 90° and 63.0% higher than at 45° for both displacement rates on the average. Statistically, loading direction had a significant effect ($p<0.05$) on the energy absorbed in the bone-tendon junction. Again, no significant interaction was found between displacement rates ($p>0.05$). The results of the energy absorption in tendon and at the bone-tendon junction are summarized in Fig. 7.

3.4 Linear stiffness

Figure 8 shows the linear stiffness for tendon and the bone-tendon junction tested at different loading directions and two displacement rates. There was not a significant correlation in stiffness for the tendon between loading directions ($p>0.05$), but the stiffness in the tendon was sensitive to the displacement rate. A two-way ANOVA showed a significant effect on linear stiffness ($p<0.05$) due to the displacement rate, with the 100 mm/min displacement rate having a 41% higher linear stiffness than the 10 mm/min displacement

Table 1 Shows th results of mechanical tensile tests in tendon and at the bone-tendon junction at three elbow positions (45°, 90° and 135° in flexion) and at displacement rates of 10 mm/min and 100 mm/min

Dis. rate (mm/min)	Specimens No.	Elbow angle in flexion (degree)	Ultimate tensile strength (N)	Failure strain			Energy absorption			Stiffness		
				tendon	bone	junction	tendon (N-mm)	bone (N-mm)	junction (N-mm)	tendon (N/mm)	bone (N/mm)	junction (N/mm)
10	12	45	28.1±15.3	0.08±0.03	0.002±0.0005	0.18±0.07	21.4±6.6	0.19±0.06	7.9±4.6	31.9±14.8	1083±834	61.3±18.8
	12	90	40.7±13.8	0.11±0.02	0.003±0.001	0.16±0.03	31.8±7.8	0.33±0.1	12.8±3.6	33.5±12.5	1124±270	74.3±20.7
	12	135	63.4±28.9	0.13±0.03	0.005±0.002	0.15±0.05	64.8±18.0	1.19±0.42	23.8±6.03	43.3±15.1	1134±490	117±32.8
100	12	45	40.3±25.4	0.05±0.02	0.005±0.001	0.15±0.06	14.6±4.4	0.59±0.23	6.62±1.9	69.3±29.9	1086±827	95.7±39.7
	12	90	51.3±11.7	0.07±0.03	0.004±0.001	0.14±0.05	28.3±9.6	0.76±0.22	11.6±2.7	52.0±12.4	1667±739	126±24.3
	12	135	76.2±28.8	0.09±0.04	0.003±0.002	0.11±0.02	46.5±18.9	0.81±0.31	16.6±6.83	60.7±28.4	1758±744	159±44.1

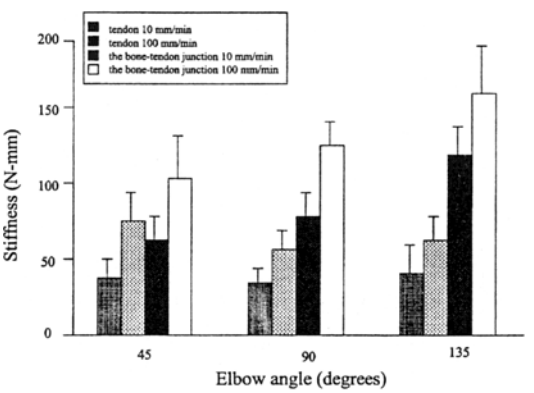

Fig. 8 Linear stiffness in tendon and at the bone-tendon junction at different loading directions and displacement rates

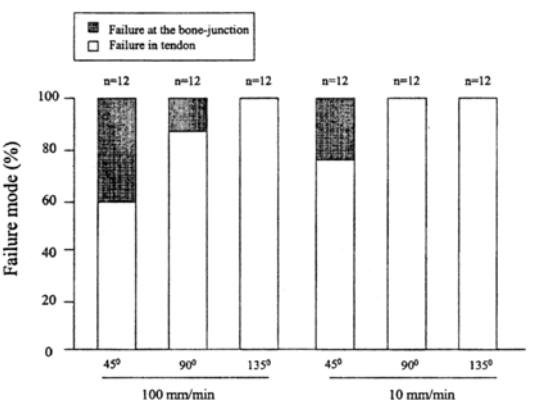

Fig. 9 Percentage of failure mode in the bone-tendon specimen

rate.

Both loading direction and displacement rate had a significant effect ($p<0.05$) on the linear stiffness for the bone-tendon junction. For specimens tested with different loading directions (45°, 90° and 135°) at the 10 mm/min displacement rate, the values of linear stiffness in the bone-tendon junction were 61.3±18.9 N/mm, 74.3 ±20.7 N/mm and 117.5±32.8 N/mm for bone-tendon specimens, respectively. At the 100 mm/min displacement rate, these values increased to 95.7±39.8 N/mm, 126.5±24.3 N/mm, and 159.6 ±44.1 N/mm, respectively. The linear stiffness for the bone-tendon junction at the 100 mm/min displacement rate was 35.9% (45°) 41.2% (90°) and 26.4% (135°) higher than those tested at the 1- mm/min displacement rate.

Table 1 lists the ultimate tensile strength for the bone-tendon specimens and details the failure strains, energy absorption and linear stiffness for the tendon and the bone-tendon junction at 45°, 90° and 135° of loading at two displacement rates.

3.5 Failure mode

The bone-tendon specimens in tensile tests showed two failure modes: tendon failure and failure at the bone-tendon junction without bone avulsion. All specimens at 135° and most specimens at 90° showed a tendon failure for both displacement rates. At 45°, 20% and 40% of specimens failed at the bone-tendon junction at the 10 mm/min and 100 mm/min displacement rates, respectively (Fig. 9). The difference in mode of failure between the 45° loading direction and the other two loading directions was statistically significant ($p<0.05$).

4. Discussion

The use of DVRTs and the video measurement system provides a technical improvement in the difficult problem of characterization of mechanical properties of the tendon, bone and bone-tendon junction. In particular, the present apparatus measures the strains of the tendon and bone without interfering with tendon sheath between fibers and into bone did not damage the tendon fibers and bone structures (Wang et., 1995). In this respect, the data obtained should prove to be closer to actual tendon and bone strain.

The DVRTs and video measurement system also eliminate the difficult problem of defining the length of the tendon, a parameter needed to determine tensile strain. For the common extensor tendon of the humeral epicondyle, initial length is difficult to define because the bone-tendon junction covers an irregular area relative to length. An incorrect initial length of the tendon would lead to incorrect calculation of tendon strain. Using the DVRTs and video measurement system, however, the tensile strain in tendon, bone and bone-tendon complex can be based on the initial gauge length the DVRTs and the distance between the two parallel ultra fine wires. The strain at the bone-tendon junction is calculated based on the strains in tendon, bone and bone-tendon complex obtained from DVRT video measurements. Therefore, the strain at the bone-tendon junction is dependent on the accuracy of strains in tendon, bone and bone-tendon complex.

This study of tensile testing of the bone-tendon specimens of the humeral epicondyle has identified two important factors that influence the structural properties of the rabbit bone-tendon unit-loading direction and displacement rate. The increases in ultimate tensile strength of the bone-tendon specimen with increasing elbow angles are similar to the previous findings by Wang, et al. (1995). The effect of ultimate tensile strength may not be due to the tendon because linear stiffness of the tendon is almost constant in all loading directions. The higher ultimate tensile strength at 135° than at 90° and 45° may relate structural properties of the bone-tendon junction. We found the lowest failure strain, highest energy absorption and highest linear stiffness in the bone-tendon junction at 135°. These results indicate that the bone-tendon junction increases its hardness or strength with an increase in elbow angle. Furthermore, the effects of loading direction on failure mode also relate to the ultimate tensile strength. At 135° and 90°, the failure mode exhibits simultaneous failure at the middle section of the tendon with an increase in ultimate tensile strength at both displacement rates. At 45°, 40% of failures occurred at the bone-tendon junction with a reduction in ultimate tensile strength. The results indicated that pure tendon rupture occurred as ultimated tensile strength increased. Decreased ultimate tensile strength results in failure occurring at the bone-tendon junction or the mode of failure becoming mixed. The general morphology of the bone-tendon junction is well known (Benjamin et al., 1986) and has been divided into four zones: tendon, unmineralized fibrocarilage, mineralized fibrocartilage and bone. The viscoelastic material and structural properties change rapidly at the bone-tendon junction (Woo et al., 1988). Therefore, tendon insertion to bone provides a means of attaching a flexible yet strong, tension-bearing structure into a rigid, noncompliant bone. The tensile forces in the tendon are thought to produce tensile, compressive and shear stresses at the bone-tendon junction (Woo et al., 1988), and the material structures of the bone-tendon junction cannot be isotropic (Currey, 1984). The differences in measured structural properties of the bone-tendon specimen are a consequence of varying the loading direction of the tendon across the bone-tendon junction. In other words, the direction of the applied force influences the force patterns at the bone-tendon junction including: tension, compressive and shear forces.

We have shown that the failure strain of the tension is consistently smaller than the failure strain calculated for the bone-tendon junction, which is similar to findings from other studies (Noyes et al., 1984; Bulter et al., 1984). These results suggest that the deformation near or at the

bone-tendon junction is larger than in the tendon. It is conceivable that large deformation near the bone-tendon junction may predispose the area to higher incidence of microfailure or microtear in tensile strength, especially in small elbow angles. For example, an increased percentage of failure occurred at the bone-tendon junction when the loading direction went from 90° to 45°.

Under the tensile loading conditions of this experiment, the bone-tendon specimens had a higher ultimate tensile strength at the 100 mm/min displacement rate than at the 10 mm/min rate. Also, lower failure strains and greater linear stiffness were found in the tendon and the bone-tendon junction at the 100 mm/min than at the 10 mm/min displacement rate. These findings dem onstrate the time-dependent behavior of the bone-tendon unit. Tendon and its insertion site are composite materials consisting of cllagen and other tissues. The collagen exhibits viscoelastic mechanical behavior (Hooley et al., 1980). Therefore, the reduction of the ultimate tensile strength in the bone-tendon unit, and increasing failure strains and decreasing linear stiffness in the tendon and at the bone-tendon junction at the 10 mm/min displacement rate were due, in part, to the creep behavior in the tendon and at the bone-tendon junction (Wang et al., 1995).

No previous study has documented the time-dependent failure properties of the bone-tendon specimens of the humeral epicondyle over a wide range of strain rates. Han et al. (1994) used two strain rates for human cadaver specimens. The results of that study showed that ultimate tensile strength was independent of strain rate. In contrast, the current study indicated that ultimate tensile strength of the bone-tendon unit, failure strain and stiffness of tendon and the bone-tendon junction depend significantly on strain rae. The difference between these two studies may be due to the different range of strain rates.

In conclusion, the direction of applied tensile load and the displacement rate should be very important parameters to consider when investigating the biomechnical properties of the bone-tendon unit of the epicondyle. Based on this study, the common extensor tendon and its insertion site on the humeral epicondyle had different mechanical responses to the testing conditions. It appears that the differences in measured ultimate tensile strength, failure strain, energy absorption and linear stiffness are a consequence of varying the loading direction and strain rate of the tendon across the bone-tendon junction. In future studies, the fatigue response to a series of elbow flexion angles will be investigated. The method of strain measurement used in this study is one of many possible ways to examine the bone-tendon unit. However, it is hoped that a better method will be designed to measure strain more accurately.

Acknowledgment

This Research was financially supported by Hansung University in the year of 2001

Reference

Armstrong, T. and Chaffin, D., 1979a, "Some Biomechanical Aspects of the Carpal Tunnel," *J. Biomech.* Vol. 12, pp. 567～570.

Butler, D. L., Grood, E. S. and Noyes, F. R., 1984, "Effects of Structure and Strain Measurement Technique on the Material Properties of Young Human Tendons and Fascia," *J. Biomech.* Vol. 17, pp. 579～596.

Castelli, W. A., Evans, F. G., Diaz-Perez, R. and Armstrong, T. J., 1980, "Intraneural Connetive Tissue Proliferation of the Median Nerve in Carpal Tunnel Syndrome," *Archs. Phys. Med. Rehabil.* Vol. 61, pp. 418～422.

Currey, J. D., 1984, "The Mechanical Adaptation of Bones," Princeton University Press. pp. 190～192.

Han, J. S., Lee, K. H., Ryu, J. and Kish, V., 1995, "Failure Strength and Pattern of Bone -Tendon Specimens of the Common Extensor and Flexor Tendons of the Humeral Epicondyle After Cyclic and Tensile Loading Test," Submitted to *J. Orthop. Res.*

Hooley, C. J. and McCrum, N. G., 1980, "The Viscoelastic Deformation of Tendon," *J.*

Biomech. Vol. 13, pp. 521~528.

Jobe, F. W. and Ciccotti, M. G., 1994, "Lateral and Medial Epicondylitis of the Elbow," *J. Am. Acad. Ortho. Surg.*, Vol. 2, pp. 1~8.

Nirschl, R. P., 1973, "Tennis Elbow," *Ortho. Clin. North. Am.*, Vol. 4, pp. 787~800.

Noyes, F. R., Butler, D. L. and Grood, E. S., 1984, "Biomechanical Analysis of Human Ligament Grafts Used in Knee-Ligament Repairs and Reconstructions," *J. Bone. Joint. Surg.*, Vol. 66A, pp. 344~352.

Wainwright, S. A., 1976, *Mechanical Design in Organisms*, Wiley, New York, N. Y.

Wang, X. T. and Ker, R. F., 1995, "Creep Rupture of Wallaby Tail Tendons," *J. Exp. Biol.* Vol. 198, pp. 831~845.

Wang, X. T., Han, J. S., Ryu, J. and Vince, K., 1995, "The Effects of Elbow Joint Angle on the Mechanical Properties of the Bone-Tendon Specimen of the Common Extensor Tendon of the Humeral Epicondyle," In prepare.

Woo, S. L-Y., Hollis, J. M., Adams, D. J., Lyon, R. M. and Takai, S., 1998, "Ligament, Tendon and Joint Capsule Insertions to Bone, In "Injury and repair of the Musculoskeletal Soft Tissue," Ed. Woo, S. L-Y. and Buckwaltr, J. A., Park ridge, Illinois, American Academy of Orthopedic Surgeon, pp. 133~166.